

# Supporting Information

Zhou et al. 10.1073/pnas.1104150108

## SI Materials and Methods

**Electrophysiology and Data Analysis.** K<sup>+</sup> currents were recorded from inside-out patches (1) with an Axopatch 200B amplifier (Molecular Devices) and low-pass filtered at 10 kHz with an integral four-pole Bessel filter. Signals were digitized with a Digidata 1322A data acquisition system (Molecular Devices) at 100 kHz. The recordings were controlled by the pClamp 9.2 software suite (Molecular Devices). All experiments were performed at room temperature (21–24 °C).

The access resistance of recording electrodes was in the range of 0.8 to 2 MΩ after fire-polishing and filling with pipette solution containing (in mM): 140 potassium methanesulfonate, 20 KOH, 10 Hepes, 2 MgCl<sub>2</sub> (pH 7.0). Ca<sup>2+</sup> and reagents were applied onto patches through bath solution by using an SF-77B fast perfusion stepper system (Warner Instruments). The standard bath solution (cytosolic side of patch) contained (in mM): 140 potassium methanesulfonate, 20 KOH, 10 Hepes (pH 7.0). Solutions with various [Ca<sup>2+</sup>] were prepared as described before (2). The stock solutions of MTS reagents were prepared by dissolving TR-MTSEA in DMSO at 20 mM and all other MTS reagents in water at 100 mM. Stock solutions were stored at –20 °C. For experiments using MTS reagents, aliquots of stock solution were thawed and diluted to the desired concentration in bath solution immediately before application.

Single channel data were analyzed with pClamp 9.2. The G–V relationship of BK currents was constructed from isochronal tail current measured at 100 μs after variable test steps. The G–V curve was fit with the Boltzmann function to determine the potential for half-maximal activation (V<sub>h</sub>) and apparent equivalent gating charge (z):

$$G(V) = \frac{G_{\max}}{1 + \exp\left(\frac{zF(V_h - V)}{RT}\right)}, \quad [\text{S1}]$$

where *F*, *R*, and *T* have their usual physical meanings. The difference in Gibbs free energy between closed and open states at 0 mV (Δ*G*<sub>0</sub>) was further determined as follows:

$$\Delta G_0 = 0.2389zFV_h. \quad [\text{S2}]$$

The change in Δ*G*<sub>0</sub> caused by cysteine mutation at each site can be then be calculated as follows:

$$\Delta\Delta G_0 = \Delta G_0^{\text{mut}} - \Delta G_0^{\text{BG}}. \quad [\text{S3}]$$

The periodicity of ΔΔ*G*<sub>0</sub> for mutations was analyzed by Fourier transform methods (3, 4) according to the following equations:

$$\begin{aligned} P(\omega) &= \left( X(\omega)^2 + Y(\omega)^2 \right) \\ X(\omega) &= \sum_{j=1}^n \left( (V_j - \bar{V}) \sin(j\omega) \right) \\ Y(\omega) &= \sum_{j=1}^n \left( (V_j - \bar{V}) \cos(j\omega) \right), \end{aligned} \quad [\text{S4, S5, and S6}]$$

where *P*(*ω*) is the Fourier transform spectrum as a function of angular frequency *ω*, *n* is the number of residues in the helix, *V*<sub>*j*</sub> is the ΔΔ*G*<sub>0</sub> at a given position *j*, and *V*<sub>̄</sub> is the mean value of |ΔΔ*G*<sub>0</sub>| for the segment. The power spectrum of an ideal amphipathic α-helix with 3.6 residues per turn should peak at approximately 100°. However, transmembrane helices tend to peak at higher angular frequency of approximately 105° (4–6).

To quantitatively evaluate the α-helical character of a given segment, the αPI (3, 4) was calculated as a weighted area within a given frequency range (for α-helices, the range is between 80° and 120°), relative to the area of the entire power spectrum according to the following:

$$\alpha PI = \frac{\frac{1}{30^\circ} \int_{90^\circ}^{120^\circ} P(\omega) d\omega}{\frac{1}{180^\circ} \int_{0^\circ}^{180^\circ} P(\omega) d\omega}, \quad [\text{S7}]$$

An αPI value greater than 2 is considered indicative of α-helix (3, 6).

Statistical analysis and curve fitting were performed with OriginPro 7.5 (OriginLab). Mean values are presented as mean ± SEM.

1. Hamill OP, Marty A, Neher E, Sakmann B, Sigworth FJ (1981) Improved patch-clamp techniques for high-resolution current recording from cells and cell-free membrane patches. *Pflugers Arch* 391:85–100.
2. Zhang X, Solaro CR, Lingle CJ (2001) Allosteric regulation of BK channel gating by Ca(2+) and Mg(2+) through a nonselective, low affinity divalent cation site. *J Gen Physiol* 118: 607–636.
3. Cornette JL, et al. (1987) Hydrophobicity scales and computational techniques for detecting amphipathic structures in proteins. *J Mol Biol* 195:659–685.

4. Komiya H, Yeates TO, Rees DC, Allen JP, Feher G (1988) Structure of the reaction center from *Rhodobacter sphaeroides* R-26 and 2.4.1: Symmetry relations and sequence comparisons between different species. *Proc Natl Acad Sci USA* 85:9012–9016.
5. Li-Smerin Y, Swartz KJ (2001) Helical structure of the COOH terminus of S3 and its contribution to the gating modifier toxin receptor in voltage-gated ion channels. *J Gen Physiol* 117:205–218.
6. Rees DC, Komiya H, Yeates TO, Allen JP, Feher G (1989) The bacterial photosynthetic reaction center as a model for membrane proteins. *Annu Rev Biochem* 58:607–633.

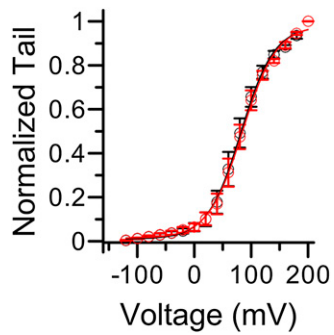


**Fig. S1.** The G-Vs of mSlo1C430S in  $10 \mu\text{M Ca}^{2+}$  before (black) and after (red) perfusion in  $500 \mu\text{M MTSET}$  for 1 min. Boltzmann fit results (line) are as follows:  $z_b = 0.86$ ,  $V_h = 82 \text{ mV}$  (before);  $z_b = 0.85$ ,  $V_h = 85 \text{ mV}$  (after).

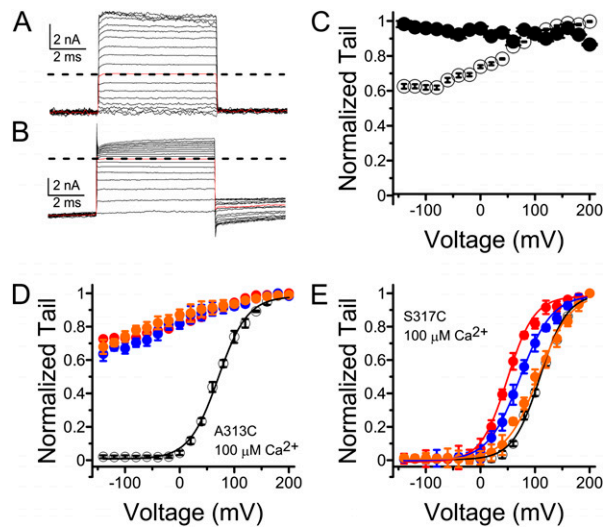


**Fig. S2.** Macroscopic currents of (A) L312C and (B) MTSET-modified A313C induced by test commands from  $-140$  to  $200 \text{ mV}$  in  $0\text{-Ca}^{2+}$  solution. Dotted line marks the zero-current level. (C) G-V relationships of MTSET-modified A313C (open circles) and L312C (filled circles) in  $0 \mu\text{M Ca}^{2+}$ . (D) G-V relationships of A313C in  $100 \mu\text{M Ca}^{2+}$  before (open circles) and after modification by MTSET (filled red circles), MTSEA (filled blue circles), or MTSES (filled orange circles). (E) G-V relationships of S317C in  $100 \mu\text{M Ca}^{2+}$  before (open circles) and after modification by MTSET (filled red circles), MTSEA (filled blue circles), or MTSES (filled orange circles).

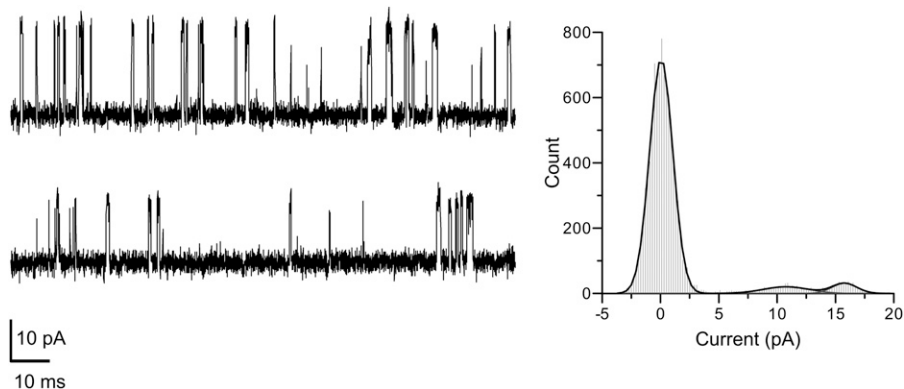


**Fig. S3.** A316C was conductive after modification by MTSACE. *Left:* Single-channel current of A316C perfused in  $50 \mu\text{M MTSACE}$  and  $300 \mu\text{M Ca}^{2+}$  at  $60 \text{ mV}$ . *Right:* All-point histogram of this recording. The single-channel conductance measurements of the channel before and after modification were  $250 \text{ pS}$  and  $167 \text{ pS}$ , respectively.

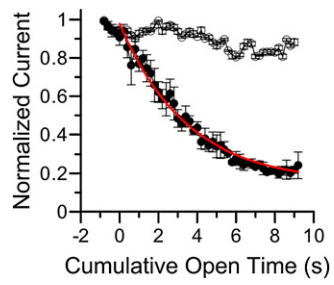


**Fig. 54.** A313C can be modified by TR-MTSEA. Figure shows the average time courses of TR-MTSEA treatment on A313C (filled circles,  $n = 3$ ) and background channels (open circles,  $n = 3$ ). Patches were perfused in  $300 \mu\text{M Ca}^{2+}$  and  $100 \mu\text{M TR-MTSEA}$ . Every second, channels were activated by a  $120 \text{ mV}$  command pulse of  $200 \text{ ms}$  duration. The red line is the single exponential fit of the modification time course of A313C by TR-MTSEA. The resulting time constant is  $3.46 \text{ s}$ , which gives a second-order modification rate of  $2.9 \times 10^3 \text{ M}^{-1}\text{s}^{-1}$ .